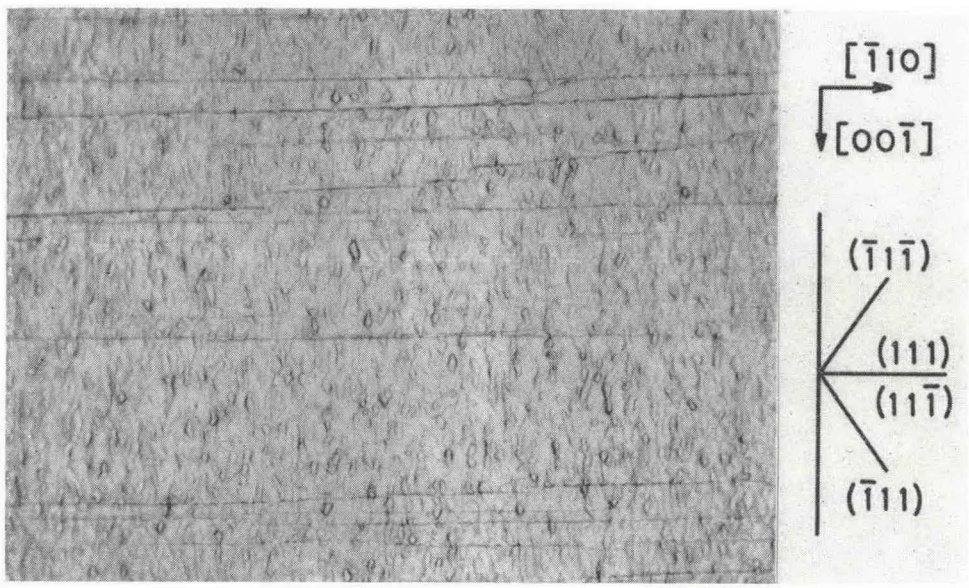

FIG. 7. Top surface of (110) [$\bar{1}$10] aluminum crystal after 24% thickness reduction, showing absence of deformation bands. Slip plane traces are noted in margin. × 280

With regard to crystal 7, (111)[$\bar{1}\bar{1}$2], the lower hardening may result from lattice reorientation, again lowering the M value. Brick and Williamson[11] have found that a (111)[$\bar{1}\bar{1}$2) brass crystal rotates to a (110)[001] position after an 80% reduction by rolling. It may be noted that $M = \sqrt{6}$ for (110)[001], which is smaller that the value of $M = 3\sqrt{6}/2$ for (111)[$\bar{1}\bar{1}$2]. Hence if lattice rotation did not occur in the present (111)[$\bar{1}\bar{1}$2] sample, use of a smaller value of M would have raised its τ–γ curve in Fig. 5. Using hardness measurements, Brick and Williamson[11] also noted a softening in their (111)[$\bar{1}\bar{1}$2] brass crystal.

Secondly, the two polycrystalline samples, 8 and 9, fall within the single crystal group. However, they do lie near the top of the list, suggesting a grain size strengthening effect not accounted for in the basic theory. (If a value of $M = 1.35\sqrt{6}$ as derived by Bishop and Hill[4] is used (see Ref. 7) instead of

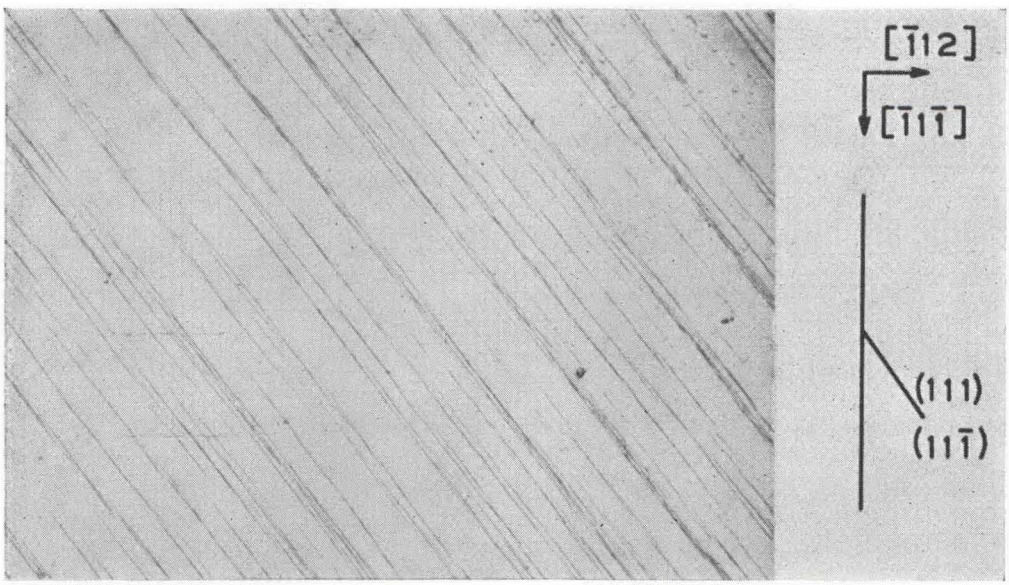

FIG. 8. Top surface of (110)[$\bar{1}$12] Permalloy crystal after 50.5% thickness reduction, electropolished, and then further deformed lightly. No constraint on ε_{yz}. Slip plane traces consistent with predicted $-a_2$, (111)[10$\bar{1}$], and b_2, (11$\bar{1}$)[011] slips. × 140

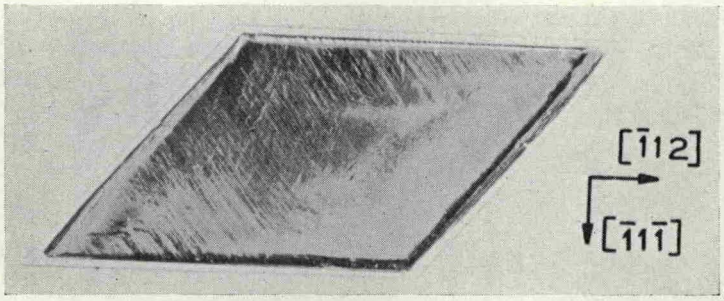

FIG. 9. Top view of (110)[$\bar{1}$12] Permalloy crystal of Fig. 8 after 50.5% thickness reduction. Transformation of the initially rectangular shape to a parallelogram indicated presence of ε_{yz}. × 2.70

$M = 1.44\sqrt{6}$ for the present study, the τ–γ curves would lie higher still. This would accentuate the possible grain size strengthening effect even more.) It may be noted that the difference between samples 8 and 9 in the cooling rate. Sample 8, slowly cooled after a 1000°C anneal, has a much higher yield stress probably as a result of ordering.

Finally, in the case of (110)[$\bar{1}$12] straining (crystal No. 2), a value of $M = \sqrt{6}$ was used in Fig. 5. This corresponds to the two-slip system ($-a_2$ and b_1) operation and leads to the strain equations (11), instead of activating additional slip systems ($-d_1$ and d_2) to conform with equations (6). The two-slip system operation is confirmed by metallographic observation of slip traces on the specimen surface, Fig. 8. In addition, the initially rectangular geometry is changed to a parallelogram after straining, Fig. 9, indicating the presence of the $d\varepsilon_{yz}$ term (equation (11)) associated with the predicted two-slip system operation. A detailed analysis[12] of the shape change has likewise confirmed that the deformation can be accounted for almost exclusively by the two predicted slip systems $-a_2$ and b_1.

By placing a (110)[$\bar{1}$12] crystal between rectangular polycrystalline blocks during compression, $d\varepsilon_{yz}$ was suppressed. As a result, all four slip systems ($-a_2$, b_1, $-d_1$ and d_2) were found to operate in accordance with analysis, see Fig. 10.

At first glance, the fact that $-d_1$, (1$\bar{1}$1)[011] and d_2, (1$\bar{1}$1)[$\bar{1}$01] can be activated at all seems surprising. The slip plane normal (1$\bar{1}$1) of these two slip systems is perpendicular to the compression axis (see Fig. 2) and hence the resolved shear stress is zero on this basis. In actuality, however, if the shear strain $d\varepsilon_{yz}$ resulting

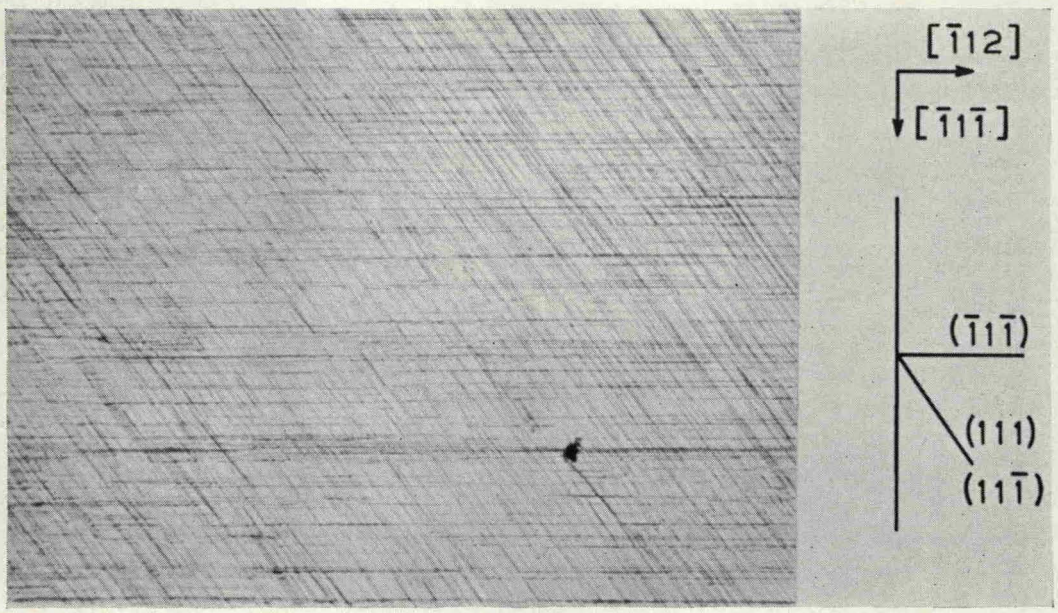

FIG. 10. Top surface of (110)[$\bar{1}$12] Permalloy crystal after 13% thickness reduction. Strain ε_{yz} was suppressed by placing the sample between polycrystalline blocks. Note additional slip traces consistent with predicted new systems $-d_1$, (1$\bar{1}$1)[011] and d_2, (1$\bar{1}$1)[10$\bar{1}$]. × 140